NURETH14-351

NUMERICAL SIMULATION OF THE FLOW IN A TIGHT LATTICE SFR ROD-BUNDLE WITH GRID SPACERS

E. Merzari[1], P. Fischer[1], D. Pointer[1], H. Ninokata[2]

[1]Argonne National Laboratory,
9700 S Cass Avenue, Lemont, IL, 60439, USA
emerzari@anl.gov
[2]Tokyo Institute of Technology,
N1-5, 2-12-1 O-okayama, Meguro-Ku, Tokyo 152-8550 Japan

Abstract

The accurate prediction of the flow in rod bundles is crucial for both the design and the safe operation of nuclear reactor systems. However the geometry complexity and the non-uniformity of the flow introduce peculiar features that can be reproduced only with three-dimensional CFD. In fact, even in bare rod bundles, i.e., bundles that do not contain any spacing device, the structure of the flow is inherently complex, due to the presence of a large-scale instability.

Moreover, experimental analysis has clearly shown that when reducing the pitch-to-diameter ratio (P/D) the turbulence field in rod bundles deviates significantly from that in a circular tube. For extremely tight configurations the existence of large-scale coherent structures has been shown, which is responsible for the high inter-sub-channel heat and momentum exchange. While there is a fairly extensive literature on the presence of these structures in bare rod-bundles and simplified geometries, there are no available studies of their presence in geometry containing grid spacers or wires.

A series of fully transient simulations of turbulence have been performed for an infinite tight triangular lattice (typical of current SFR designs) with and without a grid spacer. The simulations have been performed using Large Eddy Simulation (LES) with the spectral element code Nek5000 and unsteady Reynolds Averaged Navier-Stokes (URANS) for P/D=1.08. Several structure recognition techniques and statistical methods have been applied in order to investigate the flow field and the three-dimensional pattern of the coherent structures. The results prove that, for the configuration studied, coherent structures are indeed present and contribute significantly to the flow dynamics.

Keywords: LES, URANS, CFD, Coherent structures

1. Introduction

It is now a well established fact that the flow in rod-bundles, especially when tightly packed, differs substantially from the flow in pipes and channels [1]. Part of this complexity is due to the presence of turbulence driven secondary flows. However, the most astounding feature of rod-bundle flow is the presence of large scale coherent structures that develop in the streamwise direction in the region of the narrow gap. This gap vortex street (or gap vortex network when more than two sub-channels are involved) is due to a large scale instability (gap instability) and dominates turbulent mixing.

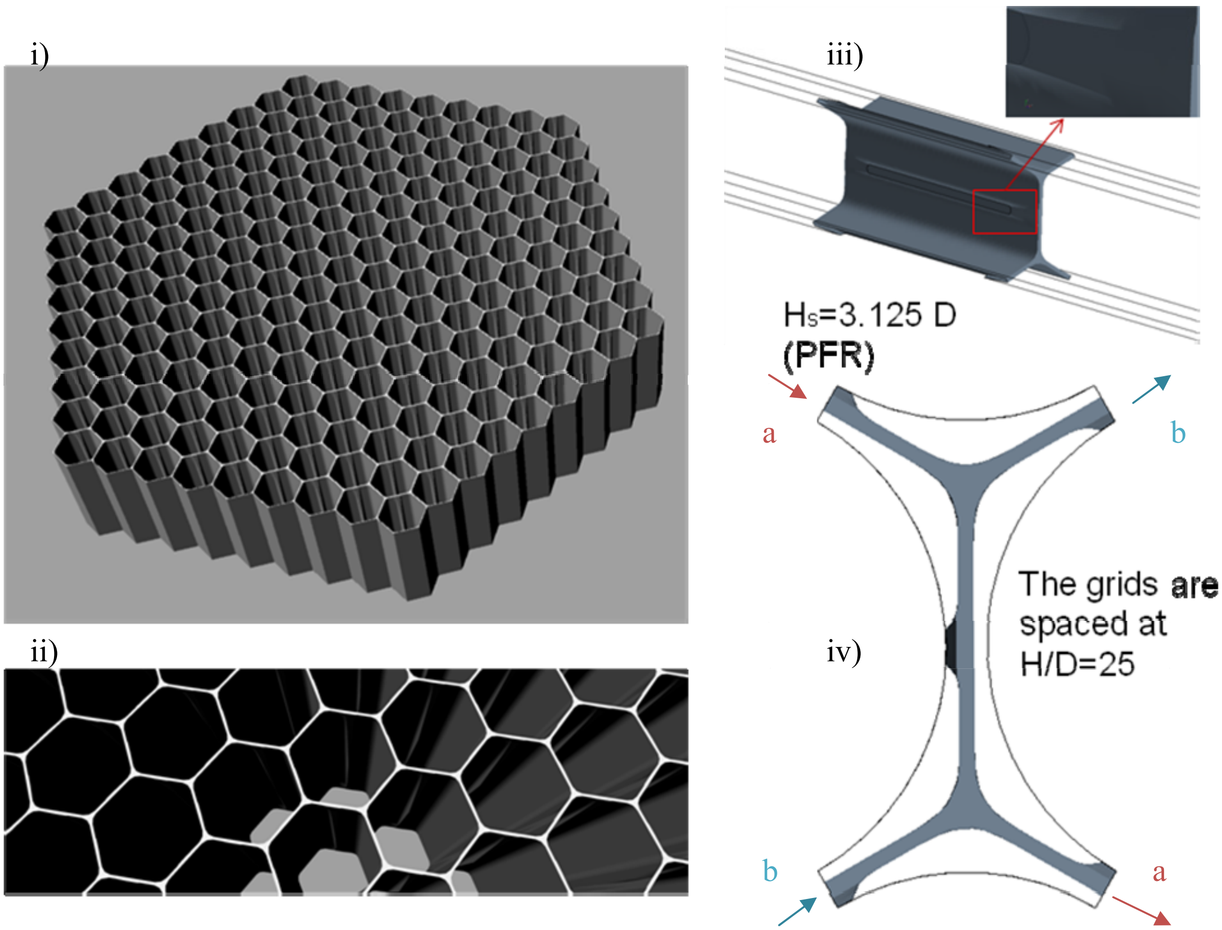

Fig. 1 Spacer grid design and boundary conditions. i) view of a 217-pin spacer grid, ii) detail, iii) view of a single pin spacer, iv) view from the top of a single pin spacer with boundary conditions

A comprehensive historical review on the subject is provided by Meyer [2], who guides the reader through the experimental discovery, the controversy and the recognition of the gap vortex street as the driver of turbulent mixing. The simulation of the vortex street has recently been achieved through CFD techniques. The first example is due to the pioneering work of Chang and Tavoularis [3], which employs Unsteady Reynolds Averaged Navier-Stokes (URANS). Several other works followed [4, 5, 6, 7] applying the same methodology, with different codes and turbulence models, to different geometries. Recently these structures have also been simulated through LES [8].

A common denominator to all the studies conducted so far, to the knowledge of the present authors, is that they rely on some form of geometric simplification. Even the most complete geometry studied [6], which consists of a significant portion of a CANDU rod bundle, does not include the spacing devices used in actual reactors. This has somewhat limited the reception of the arguments made in this introduction, since there can be reasonable doubts that the gap vortex street might survive the presence of such spacing devices.

The present paper aims to demonstrate that the gap vortex street can appear also in the presence of a large spacing device. To do so we will demonstrate that we predict coherent structures with two different codes and methodologies: the general-purpose CFD code STAR-CCM+ 5.06 and the spectral element LES code Nek5000.

The geometry investigated is a triangular lattice SFR bundle with pitch to diameter ratio equal to 1.08. This value is consistent with values that are looked upon for long-life reactor cores. Typically SFR bundles are spaced using wire-wrappers. However a minority of these reactors (among which the PFR) are spaced through grid-spacers.

In this paper a bare bundle and a grid spaced rod bundle will be examined. A three-dimensional representation of the spacers used can be found in Fig. 1. They consist of honeycomb grids 3.125 pin diameters in length, in contact with each pin through a cosine shaped dimple. In the present case the grids are separated by 25 pin diameters. In the cross section the blockage ratio reaches 40 % of the flow area in the region of the spacers.

The Geometry and the Reynolds number (*Re*=15,000) are consistent with current designs proposed for small, modular, long-life SFR cores [9].

The present paper is somewhat intentionally limited in scope. It is not our objective to fully characterize the flow in this geometry but rather to provide compelling evidence that a gap vortex street can indeed be established in a tight lattice rod-bundle containing a spacing device. Moreover, due to the strong dependency of the grid spacer design upon the reactor type, the conclusions drawn here will be limited to tight lattice SFR cores.

2. Methodology

The spacers are typically far apart: this implies that the minimum computational domain is fairly large. In order to save on the computational cost a single pin and a single span are simulated. Periodic boundary conditions in the cross section (a-a, b-b in Fig. 1iv) and in the streamwise direction are therefore used. This corresponds to an infinite triangular pitch lattice, and it is consistent with the methodology used in Merzari et al. [4], which has already demonstrated the capability to reproduce the gap vortex street in bare rod bundles for a tighter lattice (P/D=1.06).

Periodic boundary conditions introduce numerical issues (discussed in Merzari et al. [4]) that may pose issues of accuracy for the estimation of the structure size and dominant frequencies. However let us reiterate that in the present work we do not aim to characterize the gap vortex network but, rather, demonstrate it can survive the presence of a grid spacer.

At first a steady state bare rod bundle calculation was performed. Then two unsteady calculations (a URANS calculation and an LES calculation) were performed for the spacer grid case.

The methods employed for each calculation are described in the following.

2.1 URANS

The URANS calculation was performed with STAR-CCM+ 5.06. A non-linear realizable k-ε model [10] with a cubic strain-stresses algebraic relationship has been used to simulate the flow field. The wall treatment used is a Low-Reynolds approach, which is appropriate for the present low Reynolds number. A prismatic layer with 12 levels has been used to model the boundary layer. The mesh in the bulk is polyhedral (Fig. 2), and over 12 millions mesh elements have been used. The smallest y+ identified in the simulation is below $y^+=1$ and the growth rate in the prismatic layer is equal to 1.2. A preliminary steady-state calculation was used as an initial condition. An unsteady simulation was then run with a segregated solver, second order time and space discretization and a time step equal to 0.001 s. Time averaged statistics were then collected after the system reached a quasi-ergodic state. `

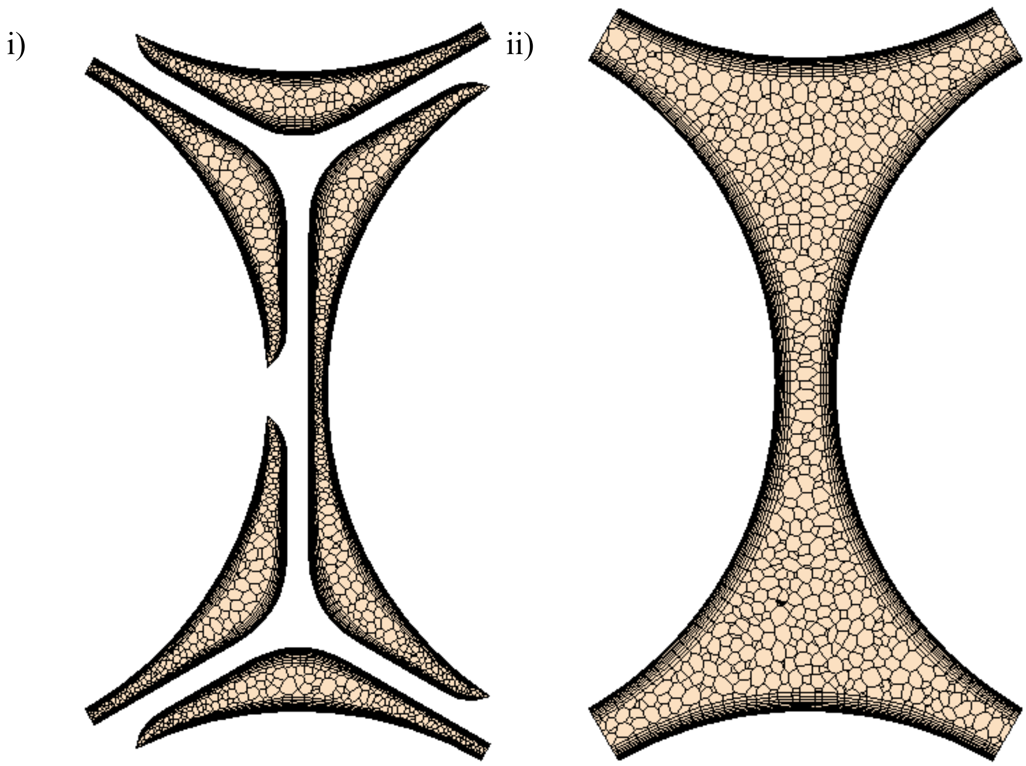

Fig. 2. Mesh for the URANS case, i) mesh in the spacer region, ii) mesh far from the spacer

2.2 LES

The simulations were carried out by using the spectral element code Nek5000 [11] on the Argonne computer systems Blue Gene/P (an IBM system with 40,960 quad-core compute nodes)—with up to 33,000,000 collocation points. An example of grid used is shown in Fig. 3 for the streamwise-normal cross section in the region of the spacers; the figure depicts the elements and the actual collocation points for the coarse mesh. The discretization is designed to allow for at least one point near the wall at $y^+<1$ and five points within $y^+<10$. For coding simplicity the domain has been rearranged in a hexagonal domain with 3 periodic sets of boundary conditions (marked on Fig. 3ii) in the cross section. The equivalence between the two domains was discussed in Ninokata et al. [12].

Spectral elements methods are a class of higher-order methods in space. Polynomial functions of up to the 7th degree have been used to discretize the velocity field in each element. In the generalized weighted residual framework, the present spectral element method can be classified as a Galerkin method where the test functions and the basis functions for each element are Lagrange polynomials evaluated on Gauss-Lobatto-Legendre collocations points (for the velocity).

In LES, large-scale turbulence is simulated while smaller scales are modeled. Since smaller scales have a nearly universal behaviour, LES is a more reliable methodology than is Reynolds-averaged Navier-Stokes (RANS), in the sense that it generally depends less on the model details. It is also preferable to use in place of direct numerical simulation because it can be performed at a reasonable computational cost.

The contribution of the smaller scales to the energy cascade is in the present case modeled through a local, element-based explicit cut-off filter in wave-number space. The energy is removed from the smallest simulated scales (high wave-numbers), thus mimicking the effect of smaller eddies [13]. This procedure allows for a coarser grid and therefore lower computational cost. Time advancement has been carried out through the characteristics method [14], which allows for higher Courant numbers to be reached. The Nek5000 code has been extensively validated and is massively parallel.

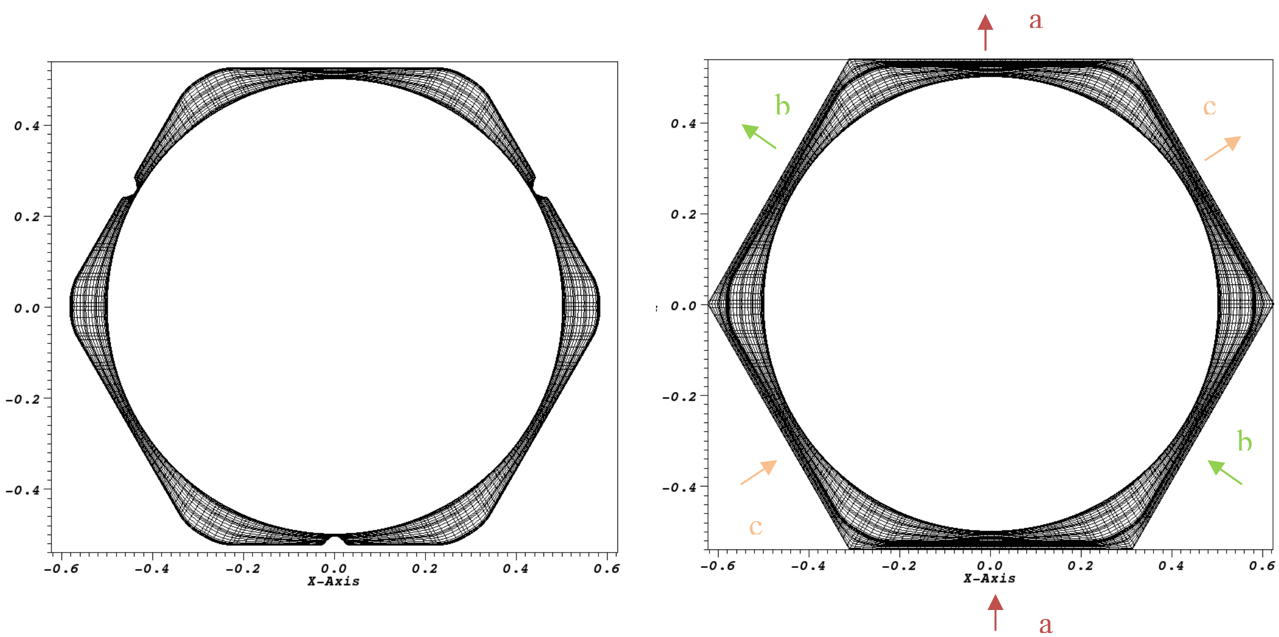

Fig. 3. Mesh for the LES case i) region of the spacers, ii) far from the spacers (the couples a-a, b-b and c-c represent the periodic boundary conditions)

An important difference needs to be pointed out between the URANS and LES calculations performed here. In the first a convenient contact area is assumed between pin and spacer dimple. In the latter, for simplicity in the LES meshing, no contact is assumed and a nominal gap is assumed between dimple and pin. This is expected to bear no significant difference between the two simulations. A further difference between the two simulations is that the Reynolds number in the LES simulation has been kept at 6,000 to reduce the computational cost.

3. Results

In the following we will present a series of results for the URANS simulation and the LES simulation. At first however let us examine the steady state results obtained with a steady state RANS, obtained with the same methodology outlined above.

Figure 4 shows a comparison between a wire wrapped bundle, a bare bundle and a grid spaced bundle obtained in a previous work [15]. All cases were run employing the same mass flow rate and the velocity magnitudes reported here are normalized by the bulk velocity. It is possible to notice how the velocity is significantly more uniform in the wire-wrapped case (the maximum is well below 1.2 times the bulk velocity), while in the bare bundle case a strong velocity gradient can be observed in the near gap region (which ultimately causes the instability responsible for the gap vortex street to develop). The same velocity gradient can be observed in the spacer grid case, far from the spacers but in the spacer grid region a strong local peak can be observed (Fig. 4 iii). This peak is ultimately responsible for a strong pressure drop increase, which in this case has been evaluated to more than a 150% increase.

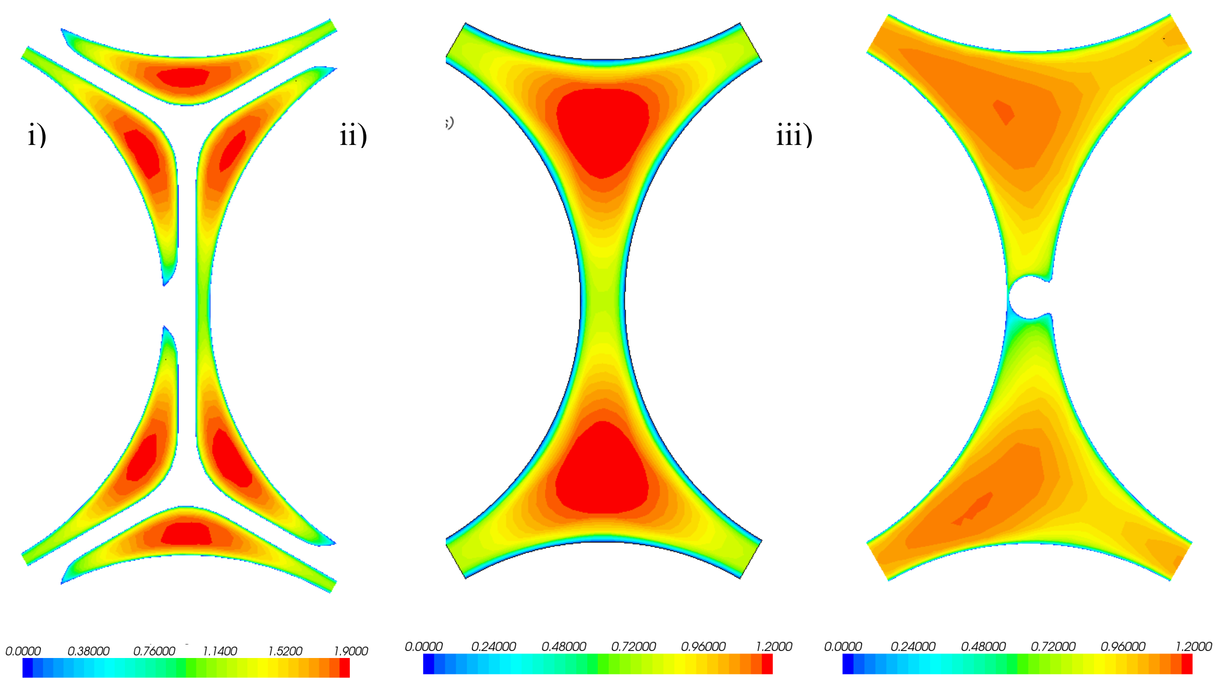

Fig. 4. Steady state results, Velocity magnitude. i) spacer grid ii) bare bundle iii) wire wrapped bundle

3.1 URANS

The URANS equations are as follows, obtained by applying the ensemble operator upon the Navier-Stokes equations.

$$\frac{\partial\langle u_i\rangle}{\partial t}+\langle u_j\rangle\frac{\partial\langle u_i\rangle}{\partial x_j}=-\frac{1}{\rho}\frac{\partial(\langle p\rangle)}{\partial x_i}-\frac{\partial}{\partial x_j}\left(\tau_{ij}-\nu\frac{\partial\langle u_i\rangle}{\partial x_j}\right), \tag{1.1}$$

$$\frac{\partial\langle u_i\rangle}{\partial x_i}=0, \tag{1.2}$$

where $\tau_{ij}=\langle u_i u_j\rangle-\langle u_i\rangle\langle u_j\rangle$ needs closure, and has been modelled through the Baglietto and Ninokata model [10].

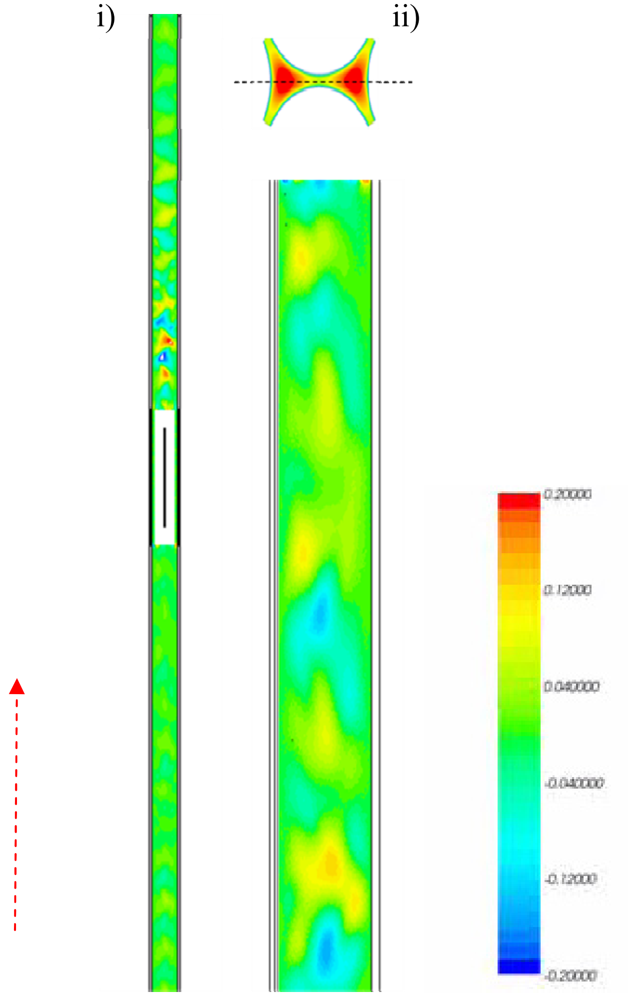

Fig. 5. URANS -Unsteady simulation, snapshot of the cross velocity for the central gap i) with detail ii). The arrow represents the flow direction

The application of averaged statistics such as the variance of the velocity components need to reflect this formulation; they can be divided in two components (a coherent part and a non-coherent part [3]):

$$c_{rms}^2 = \overline{\left\langle \left(c - \langle c \rangle\right)^2 \right\rangle} + \overline{\left(\langle c \rangle - \overline{\langle c \rangle}\right)^2} \tag{2}$$

where the term on right represents the coherent part of the stresses. The simulation rapidly develops the gap vortex street , and an oscillating cross velocity can be observed in the narrow gap, with an intensity up to 30% of the bulk velocity (Fig. 5). The intensity of the pulsation is actually increased by the presence of the spacers. And the peak of the pulsation is observed immediately downstream of the spacer (Fig. 6).

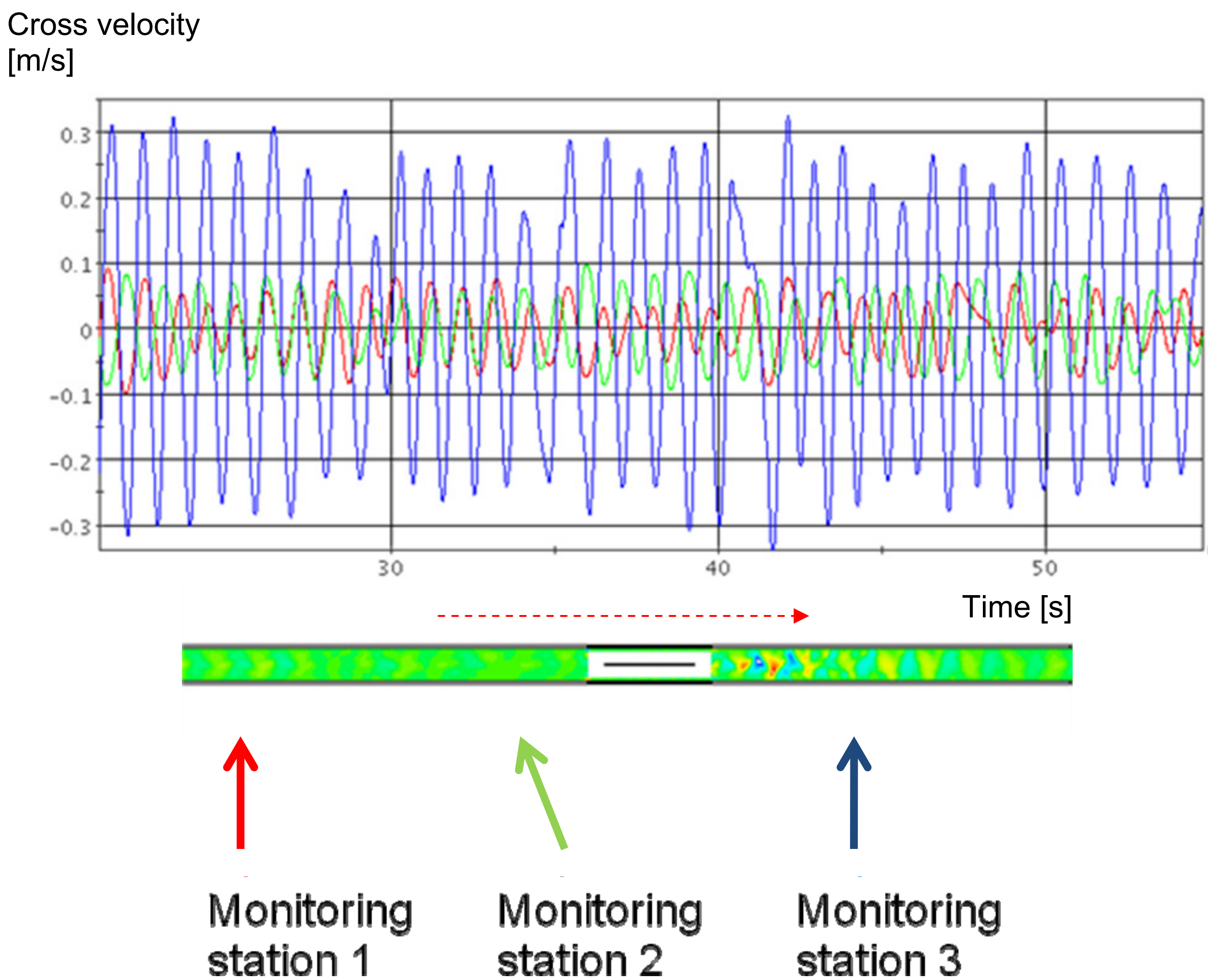

Fig. 6. URANS: Unsteady simulation, time history at three monitoring locations.

The presence of the gap vortex street strongly increases the mixing of momentum in the gap region. This can be clearly seen in the distribution of the stream-wise velocity (obtained by averaging the stream-wise velocity over a sufficient amount of time): Figure 7 shows how in the steady-state bare rod-bundle case the distribution is much less uniform than the URANS case, even far from the spacers.

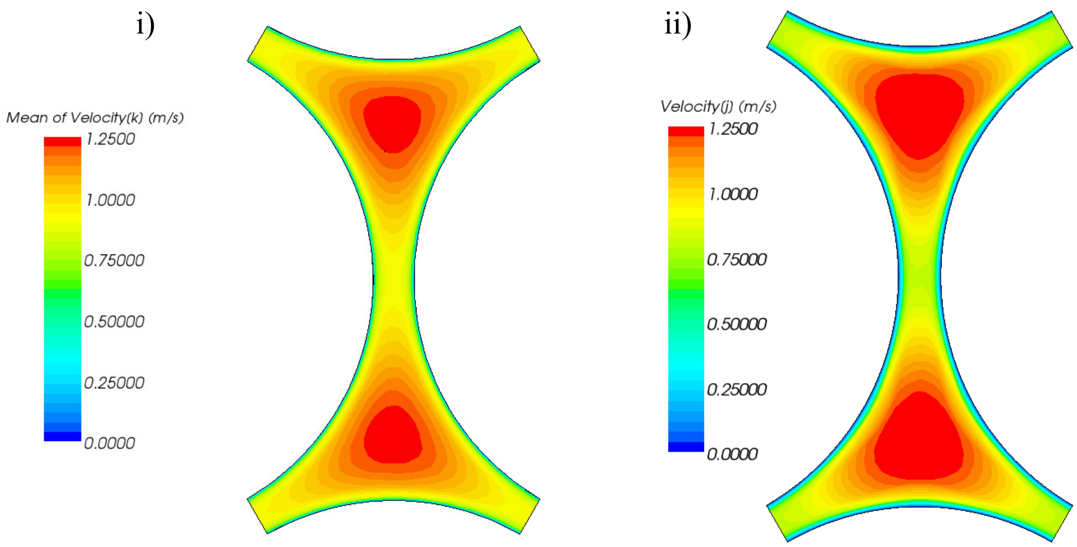

Fig. 7. Averaged URANS simulation far downstream of the spacers (i) and steady state bare bundle simulation (ii)

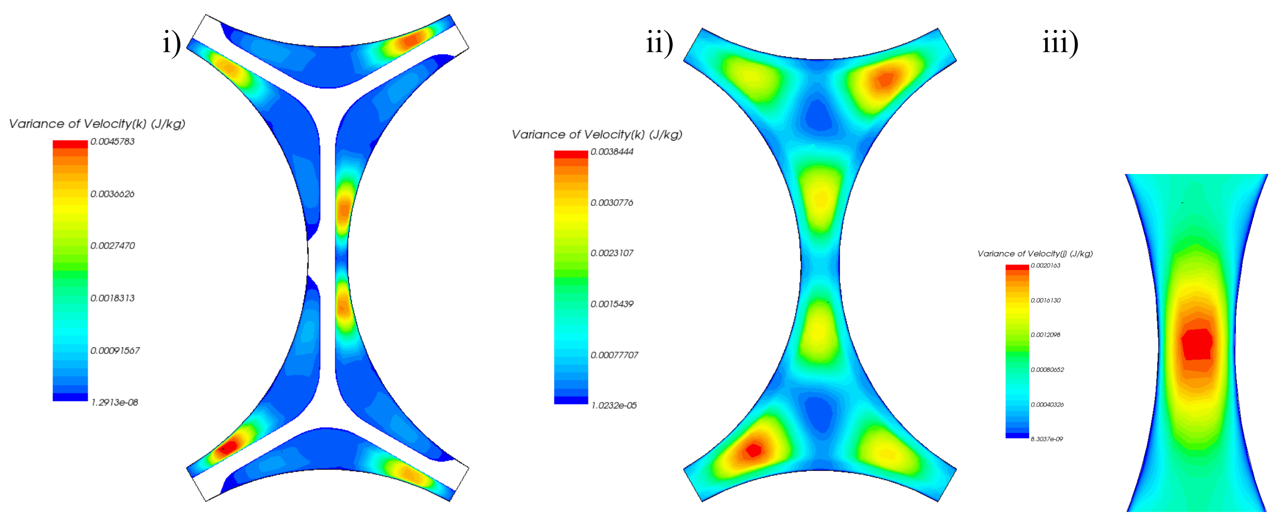

Fig. 8. URANS: Coherent component of the streamwise normal stresses in the region of the spacers (i) and far downstream (ii). Coherent component of the cross velocity variance, detail in the narrow gap region (iii)

Further characterization of the vortex street can be done by analysing the coherent part of the stresses (Fig.8). The gap vortex street is usually associated with two coherent rms peaks of the stream-wise velocity on opposite sides of the gap [5]. The two peaks can be found in Fig. 8, both in the region far from the spacers and in the spacer region. In fact in the spacer region the two peaks are preserved in the fluid portion of the domain in each of the gaps in the cross section. Moreover the peak is higher in the spacer region than outside despite the apparent breaking of symmetry due to the presence of the dimples.

The cross velocity variance has also a peak in the middle of the gap region as it can be seen in Fig. 8iii.

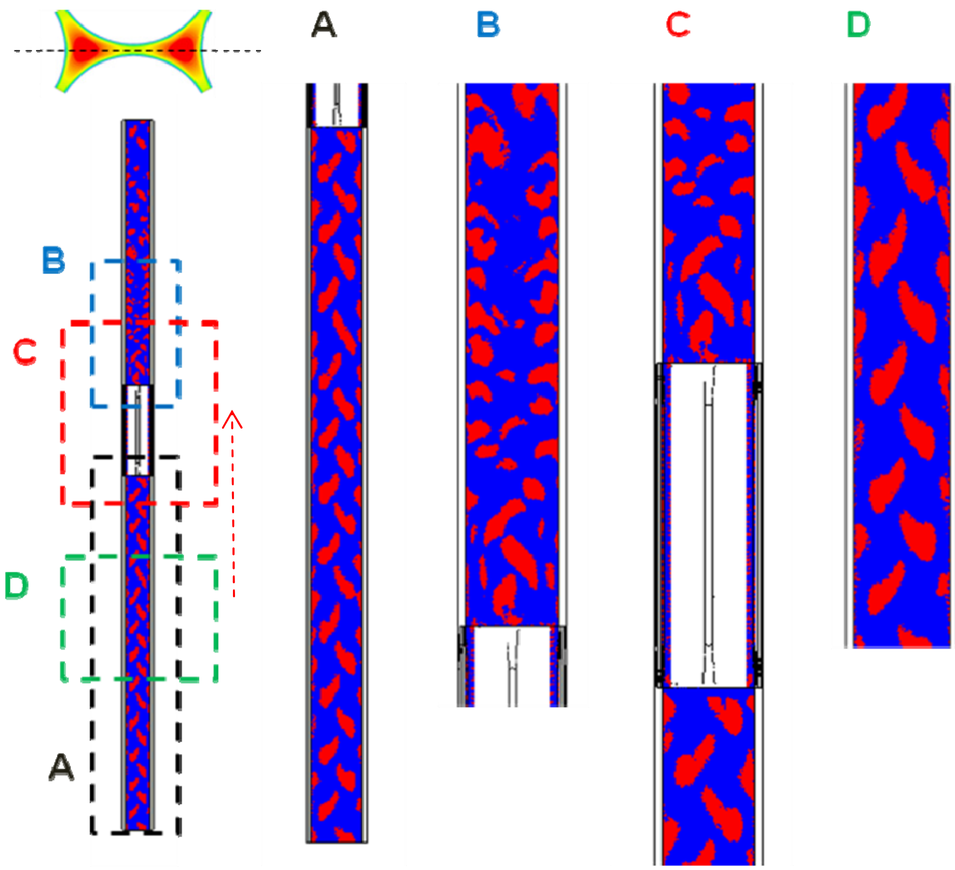

Fig. 9. URANS: Q-function plots, cross section at the mid-plane. Several views. *T=0.1*.

Further evidence of the presence of coherent structures can be found through Q-function [16] contour plots. The Q-function is the second invariant of the velocity gradient tensor and it is defined as:

$$Q = \frac{1}{2}\left(\Omega_{ij}\Omega_{ij} - S_{ij}S_{ij}\right), \tag{3}$$

where Ω_{ij} is the local rotational tensor and S_{ij} the local strain. Positive values of Q indicate regions where vorticity prevails over strain. In previous studies coherent structures have been identified as surfaces on which Q maintains a constant positive value ($Q > T$, where T is an arbitrary threshold). A series of such plots can be found in Fig. 9 which reports the Q-function on the mid-plane.

The portion of fluid in the lower part of the graph is far upstream (or downstream considering that periodic boundaries are used) of the spacer, the structure of the vortex street is best reproduced there (Fig. 9 – A, D). The vortex street is characterized by a series of coherent structures developing on each side of the gap at quasi-regular intervals. The interval at which the structures appear at a given side has been estimated at 1.08 pin diameters (the estimation is obtained by observing a series of snapshots, counting the number of structures below the spacer on a given side and dividing the total length by the total number of structures). The pattern discussed is in all similar to what has been observed in bare rod-bundles [8].

While passing through the spacer grid the coherent structures are perturbed severely (Fig. 9 – B, C) but in less than 8 pin diameters the vortex street starts recovering a coherent pattern. It appears that spacers would have to be much more closely spaced to really avoid the creation of a vortex street (less than 8 diameters apart).

3.2 LES

In this section we discuss the simulation performed with Nek5000. This simulation was performed to confirm the observations made in the URANS simulation, and in particular that a gap vortex street is established in the narrow gap region. Q-function contour plots are less effective in LES due to the presence of a large range of scales for the coherent structures, connected to wall turbulence [8].

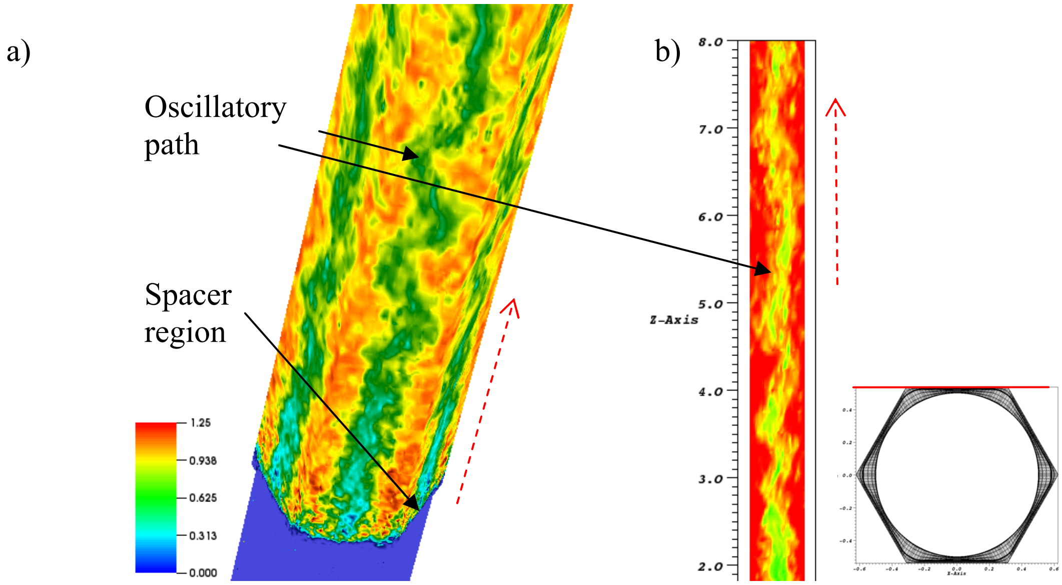

Fig. 10 LES: Velocity magnitude in the wake of the spacers. The arrows indicate respectively the spacer region and the sinusoidal path. a) 3D view, b) and narrow gap section

Figure 10 shows a snapshot of the flow field (velocity magnitude), it is possible to notice a quasi-sinusoidal path in all similar to what was observed in a rod bundle and other simplified geometry [4]. One of the key methods to identify the gap vortex street is Proper Orthogonal Decomposition (POD) [17]. It allows for the recognition of the most energetic modes of turbulence by performing an eigenvalue decomposition of the covariance matrix. Such matrix is computed according to Sirovich et al. [18]

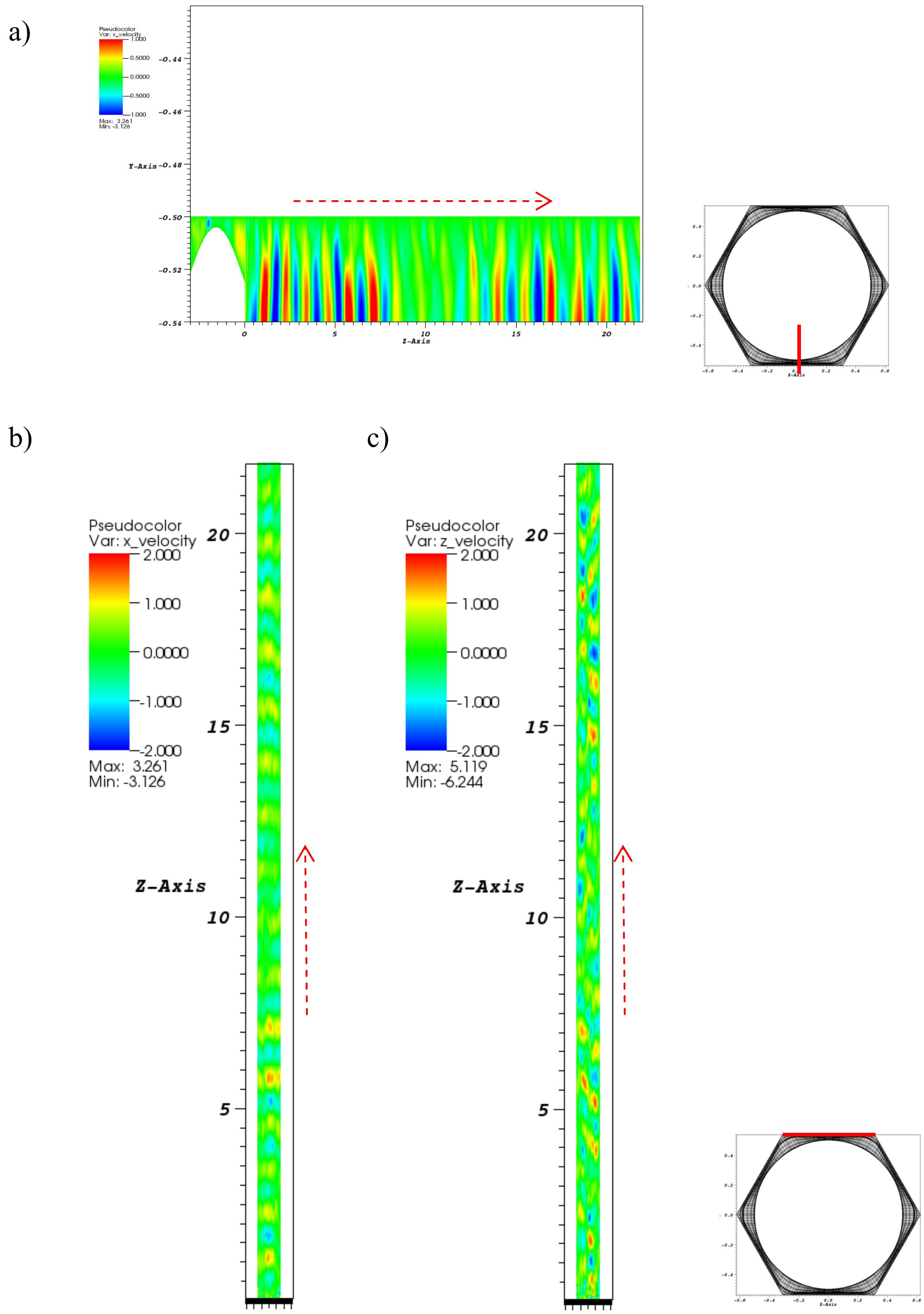

Fig. 11. POD: Most energetic eigenmode: section contour plots. a) cross velocity in the narrow gap, b) cross velocity on the upper boundary, c) streamwise velocity on the upper boundary

Merzari et al. [19] identified the modes of turbulence responsible for the gap vortex street in a bare bundle and a simplified geometry. Modes of the same type were found in the present simulation. Figure 11 shows the most energetic mode of turbulence obtained by decomposing a covariance matrix constructed from 2,000 snapshots collected at intervals of 0.0004 TOT (turn-over times). It is possible to notice the alternating pattern of the cross velocity in the narrow gap.

4. Conclusion

A URANS and an LES simulation were performed for the flow in a rod-bundle containing a grid spacer. The evidence produced by these simulations points clearly to the presence of coherent structures and in particular to a gap vortex street:

a) The flow presented alternating coherent structures on both sides of gap, identified through a Q-function method;

b) A quasi-sinusoidal cross velocity behaviour was observed in the narrow gap;

c) The coherent variance of the streamwise velocity is peaked on both sides of the gap region, the coherent variance of the cross velocity is peaked in the narrow gap;

d) The LES simulation showed the presence of a sinusoidal path for the velocity magnitude;

e) The most energetic mode of turbulence is in all similar to the ones already identified for a bare rod-bundle containing a gap vortex street.

Apparently the spacing device only perturbs the gap vortex street, but the latter recovers quickly (in 8 pin diameters). With more complex spacers, or with grids more tightly spaced it is likely that the pattern would be destroyed.

However for the present configuration, consistent with SFR designs, the gap vortex street is present. This conclusion is relevant turbulent mixing, since the amplitude of the gap vortex street is up to 30% of the bulk velocity and it should be taken into account when simulating the flow field in a rod bundle containing spacers. When using sub-channel analysis this contribution should be taken into account through appropriate models.

5. Acknowledgments

This work was completed under the auspices of the U.S. Department of Energy Office of Nuclear Energy as part of the Generation IV Energy Systems program. The submitted manuscript has been created by the University of Chicago as Operator of Argonne National Laboratory (“Argonne”) under contract No. DE-AC02-06CH11357 with the U.S. Department of Energy.

6. Nomenclature

u_i	instantaneous cartesian velocity components
x_i	cartesian coordinates
$\langle f \rangle$	ensemble averaging of the function f
f'	$f - \langle f \rangle$
$\overline{f}$	Reynolds averaging (time averaging) of the function f
S_{ij}	$= \frac{1}{2}\left(\frac{\partial u_i}{\partial x_j} + \frac{\partial u_j}{\partial x_i} \right)$
Ω_{ij}	$= \frac{1}{2}\left(\frac{\partial u_i}{\partial x_j} - \frac{\partial u_j}{\partial x_i} \right)$
r	Relative wall distance
D	Diameter
y+	Wall distance in wall units
k	Turbulent Kinetic Energy (TKE)
τ_{ij}	Reynolds Stresses
ρ	Density
ν	kinematic viscosity
Re	Reynolds number

7. References

[1] K. Rehme, The structure of turbulence in rod bundles and the implications on natural mixing between the subchannels, *Int. J. Heat Mass Transfer* **35** (1992), p. 567

[2] L. Meyer "From discovery to recognition of periodic large scale vortices in rod bundles as source of natural mixing between subchannels—A review", *Nuclear Engineering and Design*, **240**, pp. 1575-1588 (2010)

[3] D. Chang and S. Tavoularis, Unsteady numerical simulations of turbulence and coherent structures in axial flow near a narrow gap, *Trans. ASME* **127** (2005), pp. 458–466.

[4] E. Merzari, E. Baglietto and H. Ninokata, "Numerical Simulation of Tight Lattice Rod Bundles", *Nuclear Engineering and Design*, **238**, 1703-1719 (2008)

[5] D. Chang and S. Tavoularis, Convective heat transfer in turbulent flow near a gap, *J. Heat Transfer* **128** (2006), pp. 701–708.

[6] D. Chang and S. Tavoularis, Numerical simulation of turbulent flow in a 37-rod bundle, *Nucl. Eng. Des.* **237** (2007), pp. 575–590.

[7] D. Home, G. Arvanitis, M.F. Lightstone and M.S. Hamed, Simulation of flow pulsations in a twin rectangular sub-channel geometry using unsteady Reynolds Averaged Navier–Stokes model, *Nucl. Eng. Des.* **239** (2009), pp. 2964–298

[8] E. Merzari, H. Ninokata, "Proper Orthogonal Decomposition of the flow in a tight-lattice rod-bundle", *Nuclear Engineering and Deisgn*, *(in press)*

[9] N. Ueda, I. Kinoshita, A. Minato, S. Kasai, T. Yokoyama and S. Maruyama, "Sodium cooled small fast long-life reactor "4S"", *Progress in Nuclear Energy*, **47**, pp. 222-230 (2005).

[10] E. Baglietto and H.Ninokata, "Anisotropic Eddy Viscosity Modeling for Application in Industrial Engineering Internal Flows", *Int. J. Transport Phenomena*, **8** (2006)

[11] Fischer P.F., Lottes J., Pointer W.D., and Siegel A., "Petascale algorithms for reactor hydrodynamics," *J. Phys. Conf. Series* (2008)

[12] H. Ninokata, E. Merzari and A. Khakim, "Analysis of Low Reynolds Number Turbulent Flow Phenomena in Nuclear Fuel Pin Subassemblies of Tight Lattice Configuration", *Nuclear Engineering and Design*, **239**, 855-866 (2009)

[13] J.S. Mullen and P.F. Fischer, "Filter-Based Stabilization of Spectral Element Methods" *Comptes Rendus de l'Académie des sciences Paris, **332**, Série I - Analyse numérique*, 265-270 (2001)

[14] Maday Y., Patera A and Ronquist E.. "An operator-integration-factor splitting method for time dependent problems: Application to incompressible fluid flow", *Journal of Scientific Computing*, pp. 263-292 (1990)

[15] E. Merzari, J. G. Smith, W. D. Pointer, "Hydrodynamic analysis of different spacing strategies for a tight-lattice SFR bundle", *Transactions of the American Nuclear Society*, **103**, pp. 860-861 (2010)

[16] Hunt J., Wray A., Moin P., "Eddies, Streams and convergence zones in turbulent flows", Report CTR-S88, Center for turbulence Research – Stanford university (1988)

[17] G. Berkooz, P. Holmes, J.L., Lumley, The proper orthogonal decomposition in the analisys of turbulent flow, *Annual Reviews of Fluid Mechanics*, **25**, 539-575 (1993)

[18] L. Sirovich, Turbulence and the dynamics of coherent structures, Part I: Coherent structures, *Quarterly of Applied mathematics*, **XLV**, 561-571 (1987)

[19] E. Merzari, H. Ninokata, A. Mahmood, M. Rohde, "Proper Orthogonal Decomposition of the flow in geometries nontaining a narrow gap", *Theroretical and Computational Fluid Dynamics*, **23**, 333-351 (2009b)